High-power operation of electroabsorption modulators

Zhixi Bian, James Christofferson, and Ali Shakouri[a)]
Baskin School of Engineering, University of California, Santa Cruz, California 95064

Peter Kozodoy
Agility Communications Inc., Santa Barbara, California 93117

(Received 11 April 2003; accepted 8 September 2003)

Using a thermoreflectance imaging technique, surface temperature of active electroabsorption modulators is measured at different incident powers and modulator biases. Excellent agreement is obtained between these data and the results of a self-consistent finite element model. It is shown experimentally and theoretically that thermal runaway at high-power operation can be avoided by improving the thermal design of the device. High-power operation is achieved in an optimized device structure, yielding a high, damage-free power dissipation level in excess of 300 mW. [DOI: 10.1063/1.1623338]

Electroabsorption modulators (EAMs) have been widely used in fiber optic communication systems for their small size, low driving voltage, low chirp, and high bandwidth.[1,2] In addition, due to matching of material systems, EAMs can be easily integrated with other optical components, such as semiconductor lasers, semiconductor optical amplifiers, and attenuators.[3–5] Since many material properties, such as bandgap, refractive index, and thermal conductivity, change with temperature, internal heating must be considered in the design of an EAM. This is especially important for high-power operation, because large heating can damage the device. The input power tolerance of InGaAsP EAMs have been investigated experimentally in terms of breakdown phenomena, and it was shown that optical power for breakdown depended on bias voltage and operating wavelength.[6] In addition, since incident light is attenuated along the modulator, the temperature distribution is not uniform, as measured by Allard *et al.* using a liquid crystal technique.[7] The positive feedback from the interaction of absorption and temperature may make light absorption and heating greatly localized at the input of the modulator, and the peak temperature increased nonlinearly with incident light power and bias voltage. This is termed ''thermal runaway.'' In this report, we reveal the thermal runaway phenomenon by a self-consistent optoelectrothermal model and the thermoreflectance measurements. By improving the thermal design of the modulator, the thermal runaway is avoided and high-power operation is achieved in an optimized device, yielding a very high, damage-free power dissipation level in excess of 300 mW.

We measured the temperature profile in active devices using the thermoreflectance technique, which is based on the temperature dependence of the surface reflection coefficient. This thermal imaging system has achieved submicron spatial resolution and $<0.1\,^{\circ}\mathrm{C}$ temperature resolution.[8] Calibration was done using a method outlined by Dilhaire *et al.*[9] and also using microthermocouples. A thermoreflectance coefficient of $8.1\times10^{-5}/\mathrm{K}$ was obtained for the gold surface and a value of $-4.7\times10^{-5}/\mathrm{K}$ was obtained for the InP substrate material with a 100 W mercury arc lamp provided by Oriel instruments. Using these coefficients, the change in the reflection coefficient is measured and related to the surface temperature. The measurements were performed on an EA ridge modulator, which was integrated with a widely tunable semiconductor laser operating at approximately 1.55 μm. The modulator is formed of a quaternary intrinsic layer with thickness 0.4 μm, surrounded by p- and n-type InP. Figure 1 shows a picture of the modulator along with thermal images taken at a reverse bias of 2.7 V (OFF state) and 0 V (ON state). From the thermal images, light absorption and attenuation down the modulator can be seen in the OFF state.

To investigate thermal effects in the modulator, both the absorption and thermal models need to be constructed. We use the Franz–Keldysh effect described analytically by Airy functions[10] to obtain the local optical absorption coefficient. Since optical absorption generates heat, the final temperature of a biased EAM is larger than that before biasing. There are mainly two sources of heating when photons are absorbed and electron–hole pairs are generated: carrier energy relaxation inside the bands, and Joule heating due to carrier drift by the external electric field. The relaxation energy is negligible compared to the latter. Given the material absorption

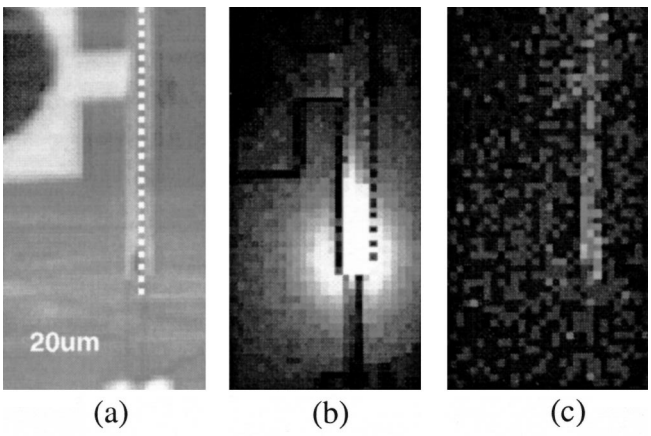

FIG. 1. (a) Optical and thermal image of an EAM biased at (b) -2.7 V and (c) 0 V. The dotted line along the modulator ridge indicates the position of the line scans used in subsequent graphs.

[a)]Author to whom correspondence should be addressed; electronic mail: ali@soe.ucsc.edu

coefficient and optical confinement of the intrinsic layer, and assuming unity quantum efficiency, the photocurrent I_{mod} can be calculated for a finite length L of modulator:

$$I_{\mathrm{mod}}=\frac{P[1-\exp(-\alpha\Gamma L)]}{\hbar\omega}q \tag{1}$$

where P is the input light power and Γ is the optical confinement of intrinsic layer. The heating from carrier drift can be derived from photocurrent and bias voltage. Once the heating Q is calculated, the temperature increase can be derived from thermal impedance of the EAM waveguide. We used a two-dimensional thermal impedance model Z_t for the ridge waveguide structure of EAM:[11]

$$Z_t=\frac{\log(4h/w)}{\pi L\xi}, \tag{2}$$

where h is the distance to ideal heat sink, w is the width of absorber, and ξ is the thermal conductivity.

It should be noted that temperature dependence enters into several terms of interest, including the absorption coefficient, the bandgap of the intrinsic layer, and the thermal conductivity of the materials. The thermal shrinkage of the bandgap of InGaAsP/InP material systems is empirically given by the Varshni equations.[12] Carrier-induced bandgap shrinkage[13] is negligible compared to the thermally induced bandgap change, and has not been included in this model. In our model, the bandgap at room temperature of the intrinsic layer is 1.5 μm in wavelength. The thermal conductivity of the semiconductor material is proportional to T^{-n}, where n is a constant between 1.375 and 1.5 for InGaAsP/InP material systems.[7] Thus, thermal impedance of the device will increase with temperature.

Thus, the four terms, absorption, waveguide temperature, thermal conductivity, and bandgap all depend on each other. In addition, since light is attenuated, light intensity, absorption, and temperature decrease down the modulator. We divided the modulator into finite one-dimensional segments, and solved the absorption and temperature in each cell by numerical iterations based on initial temperature and absorption. As the temperature rises, the bandgap decreases and the thermal impedance increases, creating a positive feedback cycle that pushes the temperature and absorption to higher values at the input of the modulator. Thermal runaway is a phenomenon at high-power operation or large bias, in which the positive feedback cycle has a significant effect. If the EAM design does not efficiently dissipate heat, this feedback cycle can lead to catastrophic device damage. To avoid thermal runaway and device breakdown at high-power operation without sacrificing the performance of the modulator, it is important to reduce the thermal resistance of the device and packaging.

In this work, two types of EAM devices were investigated. The composition and thickness of the intrinsic layer was kept constant, but two different thermal designs were employed: an unoptimized design and an optimized one. Figure 2 displays the measured surface temperature along a modulator of unoptimized thermal design for different applied voltages, compared with simulation. The thermal reflectance technique measures temperature on the surface of the device, so that the internal temperature predicted by thermal and absorption model could be slightly different. The thermal resistance of the structure has been varied as a fitting parameter in the simulation. It can be seen that a localized heating is developed in a small region on the order of 30–40 μm at the input of the modulator. Excellent agreement is obtained between the calculated and measured temperature distributions. The model is further validated by photocurrent and light throughput measurements, which are shown in Fig. 3.

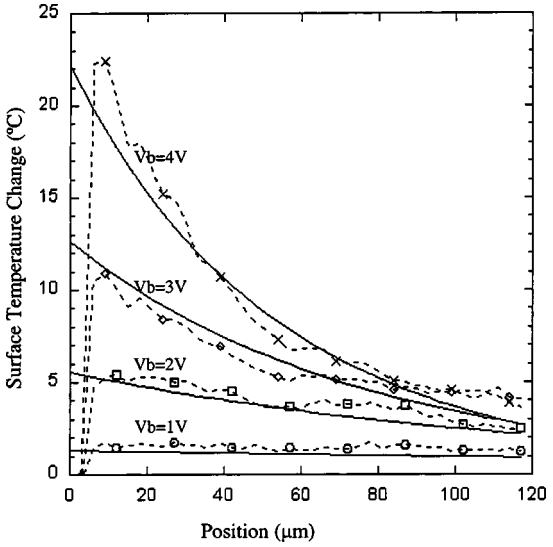

FIG. 2. Surface temperature change distribution along the modulator for different modulator bias by thermoreflectance measurement (dashed line) and by model fitting (solid line). The input power is about 6 mW and operating wavelength is 1.55 μm.

Figure 4 compares the bias dependence of peak temperature under high optical input power (35 mW) for the two different modulator designs. The unoptimized design (a) exhibits thermal runaway at a bias of 2.75 V. The EAM with improved thermal design (b) has the same modulator materials, doping, and layer structure as (a) and delivers identical

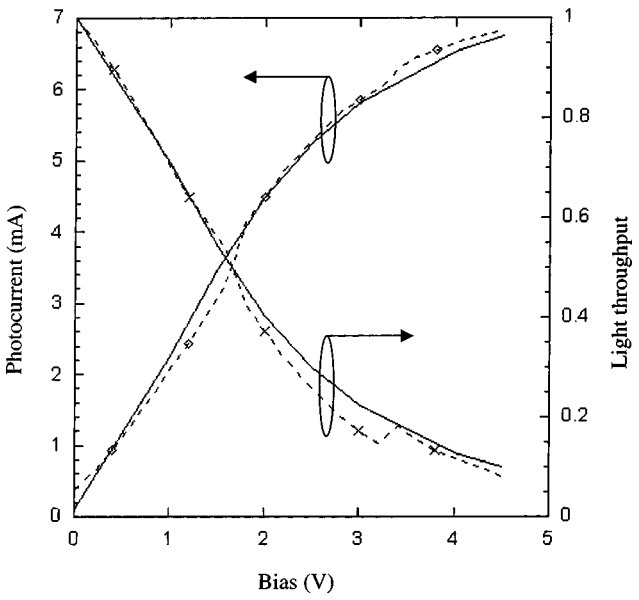

FIG. 3. Photocurrent and light throughput for different modulator bias by measurement (dashed line) and by model prediction (solid line). The input power is about 6 mW and operating wavelength is 1.55 μm.

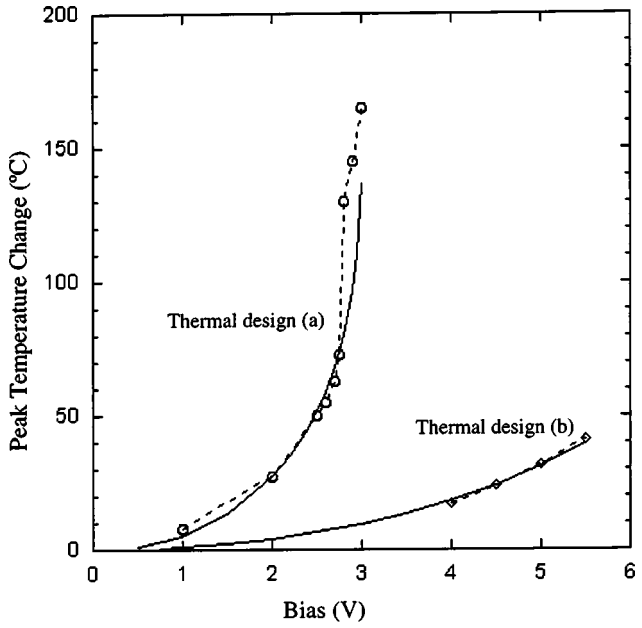

FIG. 4. Peak temperature for different modulator bias by measurement (dashed line) and by model fitting (solid line). The input power is about 35 mW and operating wavelength is 1.55 μm.

performance, but offers a much improved junction-to-the-case thermal resistance through optimization of the device geometry. It can be seen in Fig. 4 that the surface temperature is significantly reduced in this case, and that much larger voltages can be applied without triggering thermal runaway. The performance of these improved modulators was investigated in separate testing under extreme operating conditions of high optical input power and large reverse bias. The devices consistently achieve damage-free operation at a dc bias of 5V and well over 60 mA photocurrent (total electrical power in excess of 300 mW).

In conclusion, using a thermoreflectance imaging technique, surface temperature measurements of active electroabsorption modulators are acquired. Localized heating by more than 160 °C at the input of the modulator is observed under certain conditions, and is accurately simulated by a finite element model. Both experiment and model show that thermal runaway can be avoided by improving the thermal design of the device. Optimized structures show a dramatic reduction in operating temperature, and achieve a high dissipated power limit of more than 300 mW.

[1] Y.-J. Chiu, H.-F. Chou, V. Kaman, P. Abraham, and J. E. Bowers, IEEE Photonics Technol. Lett. **14**, 792 (2002).
[2] S. Irmscher, R. Lewen, and U. Eriksson, IEEE Photonics Technol. Lett. **14**, 923 (2002).
[3] B. Mason, G. A. Fish, S. P. Denbaars, and L. A. Coldren, IEEE Photonics Technol. Lett. **10**, 1256 (2002).
[4] H. Kawanishi, Y. Yamauchi, N. Mineo, Y. Shibuya, H. Murai, K. Yamada, and H. Wada, IEEE Photonics Technol. Lett. **13**, 954 (2001).
[5] R. A. Salvatore, R. T. Sahara, M. A. Bock, and I. Libenzon, IEEE J. Quantum Electron. **38**, 464 (2002).
[6] H. Tanaka, M. Horita, Y. Matsushima, and Y. Takahashi, Opt. Quantum Electron. **28**, 605 (1996).
[7] M. Allard, R. A. Masut, and M. Boudreau, J. Lightwave Technol. **18**, 813 (2000).
[8] A. Shakouri, J. Christofferson, and Z. Bian, *Photonic Devices and Systems Packaging Symposium*, Stanford, CA, July, 2002.
[9] S. Dilhaire, S. Jorez, L. D. Patino Lopez, J. C. Batsale, and W. Claeys, Heat Tansfer and Transport Phenomena in Microsystems, 392 (2000).
[10] P. K. Basu, *Theory of Optical Processes in Semiconductor: Bulk and Microstructures*, (Oxford University Press, New York, 1997).
[11] L. A. Coldren and S. W. Corzine, *Diode Lasers and Photonic Integrated Circuits* (Wiley, New York, 1995).
[12] H. Temkin, V. G. Keramidas, M. A. Pollack, and W. R. Wagner, J. Appl. Phys. **52**, 1574 (1981).
[13] B. R. Bennet, R. A. Soref, and J. A. del Alamo, IEEE J. Quantum Electron. **26**, 113 (1990).